

Sparse Nonparametric Graphical Models

John Lafferty, Han Liu and Larry Wasserman

Abstract. We present some nonparametric methods for graphical modeling. In the discrete case, where the data are binary or drawn from a finite alphabet, Markov random fields are already essentially nonparametric, since the cliques can take only a finite number of values. Continuous data are different. The Gaussian graphical model is the standard parametric model for continuous data, but it makes distributional assumptions that are often unrealistic. We discuss two approaches to building more flexible graphical models. One allows arbitrary graphs and a nonparametric extension of the Gaussian; the other uses kernel density estimation and restricts the graphs to trees and forests. Examples of both methods are presented. We also discuss possible future research directions for nonparametric graphical modeling.

Key words and phrases: Kernel density estimation, Gaussian copula, high-dimensional inference, undirected graphical model, oracle inequality, consistency.

1. INTRODUCTION

This paper presents two methods for constructing nonparametric graphical models for continuous data. In the discrete case, where the data are binary or drawn from a finite alphabet, Markov random fields or log-linear models are already essentially nonparametric, since the cliques can take only a finite number of values. Continuous data are different. The Gaussian graphical model is the standard parametric model for continuous data, but it makes distributional assumptions that are typically unrealistic. Yet few practical alternatives to the Gaussian graphical model exist, particularly for high-dimensional data. We discuss two approaches to building more flexible graphical models that exploit sparsity. These two approaches are at different extremes in the array of choices available. One allows arbitrary graphs, but makes a distributional re-

striction through the use of copulas; this is a semiparametric extension of the Gaussian. The other approach uses kernel density estimation and restricts the graphs to trees and forests; in this case the model is fully nonparametric, at the expense of structural restrictions. We describe two-step estimation methods for both approaches. We also outline some statistical theory for the methods, and compare them in some examples. This article is in part a digest of two recent research articles where these methods first appeared, Liu, Lafferty and Wasserman (2009) and Liu et al. (2011).

The methods we present here are relatively simple, and many more possibilities remain for nonparametric graphical modeling. But as we hope to demonstrate, a little nonparametricity can go a long way.

2. TWO FAMILIES OF NONPARAMETRIC GRAPHICAL MODELS

The graph of a random vector is a useful way of exploring the underlying distribution. If $X = (X_1, \dots, X_d)$ is a random vector with distribution P , then the undirected graph $G = (V, E)$ corresponding to P consists of a vertex set V and an edge set E where V has d elements, one for each variable X_i . The edge between (i, j) is excluded from E if and only if X_i is independent of X_j , given the other variables $X_{\setminus\{i,j\}} \equiv (X_s : 1 \leq s \leq d, s \neq i, j)$, written

$$(2.1) \quad X_i \perp\!\!\!\perp X_j | X_{\setminus\{i,j\}}.$$

John Lafferty is Professor, Department of Statistics and Department of Computer Science, University of Chicago, 5734 S. University Avenue, Chicago, Illinois 60637, USA (e-mail: lafferty@uchicago.edu). Han Liu is Assistant Professor, Department of Operations Research and Financial Engineering, Princeton University, Princeton, New Jersey 08544, USA (e-mail: hanliu@princeton.edu). Larry Wasserman is Professor, Department of Statistics and Machine Learning Department, Carnegie Mellon University, Pittsburgh Pennsylvania 15213, USA (e-mail: larry@stat.cmu.edu).

	Nonparanormal	Forest densities
Univariate marginals	nonparametric	nonparametric
Bivariate marginals	determined by Gaussian copula	nonparametric
Graph	unrestricted	acyclic

FIG. 1. Comparison of properties of the nonparanormal and forest-structured densities.

The general form for a (strictly positive) probability density encoded by an undirected graph G is

$$(2.2) \quad p(x) = \frac{1}{Z(f)} \exp\left(\sum_{C \in \text{Cliques}(G)} f_C(x_C)\right),$$

where the sum is over all cliques, or fully connected subsets of vertices of the graph. In general, this is what we mean by a *nonparametric graphical model*. It is the graphical model analog of the general nonparametric regression model. Model (2.2) has two main ingredients, the graph G and the functions $\{f_C\}$. However, without further assumptions, it is much too general to be practical. The main difficulty in working with such a model is the normalizing constant $Z(f)$, which cannot, in general, be efficiently computed or approximated.

In the spirit of nonparametric estimation, we can seek to impose structure on either the graph or the functions f_C in order to get a flexible and useful family of models. One approach parallels the ideas behind sparse additive models for regression. Specifically, we replace the random variable $X = (X_1, \dots, X_d)$ by the transformed random variable $f(X) = (f_1(X_1), \dots, f_d(X_d))$, and assume that $f(X)$ is multivariate Gaussian. This results in a nonparametric extension of the Normal that we call the *nonparanormal* distribution. The nonparanormal depends on the univariate functions $\{f_j\}$, and a mean μ and covariance matrix Σ , all of which are to be estimated from data. While the resulting family of distributions is much richer than the standard parametric Normal (the paranormal), the independence relations among the variables are still encoded in the precision matrix $\Omega = \Sigma^{-1}$, as we show below.

The second approach is to force the graphical structure to be a tree or forest, where each pair of vertices is connected by at most one path. Thus, we relax the distributional assumption of normality, but we restrict the allowed family of undirected graphs. The complexity of the model is then regulated by selecting the edges to include, using cross validation.

Figure 1 summarizes the tradeoffs made by these two families of models. The nonparanormal can be thought of as an extension of additive models for regression to graphical modeling. This requires estimat-

ing the univariate marginals; in the copula approach, this is done by estimating the functions $f_j(x) = \mu_j + \sigma_j \Phi^{-1}(F_j(x))$, where F_j is the distribution function for variable X_j . After estimating each f_j , we transform to (assumed) jointly Normal via $Z = (f_1(X_1), \dots, f_d(X_d))$ and then apply methods for Gaussian graphical models to estimate the graph. In this approach, the univariate marginals are fully nonparametric, and the sparsity of the model is regulated through the inverse covariance matrix, as for the graphical lasso, or “glasso” (Banerjee, El Ghaoui and d’Aspremont, 2008; Friedman, Hastie and Tibshirani, 2007).¹ The model is estimated in a two-stage procedure; first the functions f_j are estimated, and then inverse covariance matrix Ω is estimated. The high-level relationship between linear regression models, Gaussian graphical models and their extensions to additive and high-dimensional models is summarized in Figure 2.

In the forest graph approach, we restrict the graph to be acyclic, and estimate the bivariate marginals $p(x_i, x_j)$ nonparametrically. In light of equation (4.1), this yields the full nonparametric family of graphical models having acyclic graphs. Here again, the estimation procedure is two-stage; first the marginals are estimated, and then the graph is estimated. Sparsity is regulated through the edges (i, j) that are included in the forest.

Clearly these are just two tractable families within the very large space of possible nonparametric graphical models specified by equation (2.2). Many interesting research possibilities remain for novel nonparametric graphical models that make different assumptions; we discuss some possibilities in a concluding section.

¹Throughout the paper we use the term graphical lasso, or glasso, coined by Friedman, Hastie and Tibshirani (2007) to refer to the solution obtained by ℓ_1 -regularized log-likelihood under the Gaussian graphical model. This estimator goes back at least to Yuan and Lin (2007), and an iterative lasso algorithm for doing the optimization was first proposed by Banerjee, El Ghaoui and d’Aspremont (2008). In our experiments we use the R packages `glasso` (Friedman, Hastie and Tibshirani, 2007) and `huge` to implement this algorithm.

Assumptions	Dimension	Regression	Graphical models
Parametric	low	linear model	multivariate Normal
	high	lasso	graphical lasso
Nonparametric	low	additive model	nonparanormal
	high	sparse additive model	sparse nonparanormal

FIG. 2. Comparison of regression and graphical models. The nonparanormal extends additive models to the graphical model setting. Regularizing the inverse covariance leads to an extension to high dimensions, which parallels sparse additive models for regression.

We now discuss details of these two model families, beginning with the nonparanormal.

3. THE NONPARANORMAL

We say that a random vector $X = (X_1, \dots, X_d)^T$ has a *nonparanormal* distribution and write

$$X \sim NPN(\mu, \Sigma, f)$$

in case there exist functions $\{f_j\}_{j=1}^d$ such that $Z \equiv f(X) \sim N(\mu, \Sigma)$, where $f(X) = (f_1(X_1), \dots, f_d(X_d))$. When the f_j 's are monotone and differentiable, the joint probability density function of X is given by

$$\begin{aligned}
 p_X(x) &= \frac{1}{(2\pi)^{d/2} |\Sigma|^{1/2}} \\
 (3.1) \quad &\cdot \exp\left\{-\frac{1}{2}(f(x) - \mu)^T \Sigma^{-1}(f(x) - \mu)\right\} \\
 &\cdot \prod_{j=1}^d |f'_j(x_j)|,
 \end{aligned}$$

where the product term is a Jacobian.

Note that the density in (3.1) is not identifiable—we could scale each function by a constant, and scale the diagonal of Σ in the same way, and not change the density. To make the family identifiable we demand that f_j preserves marginal means and variances.

$$\begin{aligned}
 (3.2) \quad \mu_j &= \mathbb{E}(Z_j) = \mathbb{E}(X_j) \quad \text{and} \\
 \sigma_j^2 &\equiv \Sigma_{jj} = \text{Var}(Z_j) = \text{Var}(X_j).
 \end{aligned}$$

These conditions only depend on $\text{diag}(\Sigma)$, but not the full covariance matrix.

Now, let $F_j(x)$ denote the marginal distribution function of X_j . Since the component $f_j(X_j)$ is Gaussian, we have that

$$\begin{aligned}
 F_j(x) &= \mathbb{P}(X_j \leq x) \\
 &= \mathbb{P}(Z_j \leq f_j(x)) = \Phi\left(\frac{f_j(x) - \mu_j}{\sigma_j}\right)
 \end{aligned}$$

which implies that

$$(3.3) \quad f_j(x) = \mu_j + \sigma_j \Phi^{-1}(F_j(x)).$$

The form of the density in (3.1) implies that the conditional independence graph of the nonparanormal is encoded in $\Omega = \Sigma^{-1}$, as for the parametric Normal, since the density factors with respect to the graph of Ω , and therefore obeys the global Markov property of the graph.

In fact, this is true for any choice of identification restrictions; thus it is not necessary to estimate μ or σ to estimate the graph, as the following result shows.

LEMMA 3.1. *Define*

$$(3.4) \quad h_j(x) = \Phi^{-1}(F_j(x)),$$

and let Λ be the covariance matrix of $h(X)$. Then $X_j \perp\!\!\!\perp X_k | X_{\setminus\{j,k\}}$ if and only if $\Lambda_{jk}^{-1} = 0$.

PROOF. We can rewrite the covariance matrix as

$$\Sigma_{jk} = \text{Cov}(Z_j, Z_k) = \sigma_j \sigma_k \text{Cov}(h_j(X_j), h_k(X_k)).$$

Hence $\Sigma = D \Lambda D$ and

$$\Sigma^{-1} = D^{-1} \Lambda^{-1} D^{-1},$$

where D is the diagonal matrix with $\text{diag}(D) = \sigma$. The zero pattern of Λ^{-1} is therefore identical to the zero pattern of Σ^{-1} . \square

Figure 3 shows three examples of 2-dimensional nonparanormal densities. The component functions are taken to be from three different families of monotonic functions—one using power transforms, one using logistic transforms and another using sinusoids.

$$\begin{aligned}
 f_\alpha(x) &= \text{sign}(x)|x|^\alpha, \\
 g_\alpha(x) &= \lfloor x \rfloor + \frac{1}{1 + \exp\{-\alpha(x - \lfloor x \rfloor - 1/2)\}}, \\
 h_\alpha(x) &= x + \frac{\sin(\alpha x)}{\alpha}.
 \end{aligned}$$

The covariance in each case is $\Sigma = \begin{pmatrix} 1 & 0.5 \\ 0.5 & 1 \end{pmatrix}$, and the mean is $\mu = (0, 0)$. It can be seen how the concavity and number of modes of the density can change with different nonlinearities. Clearly the nonparanormal family is much richer than the Normal family.

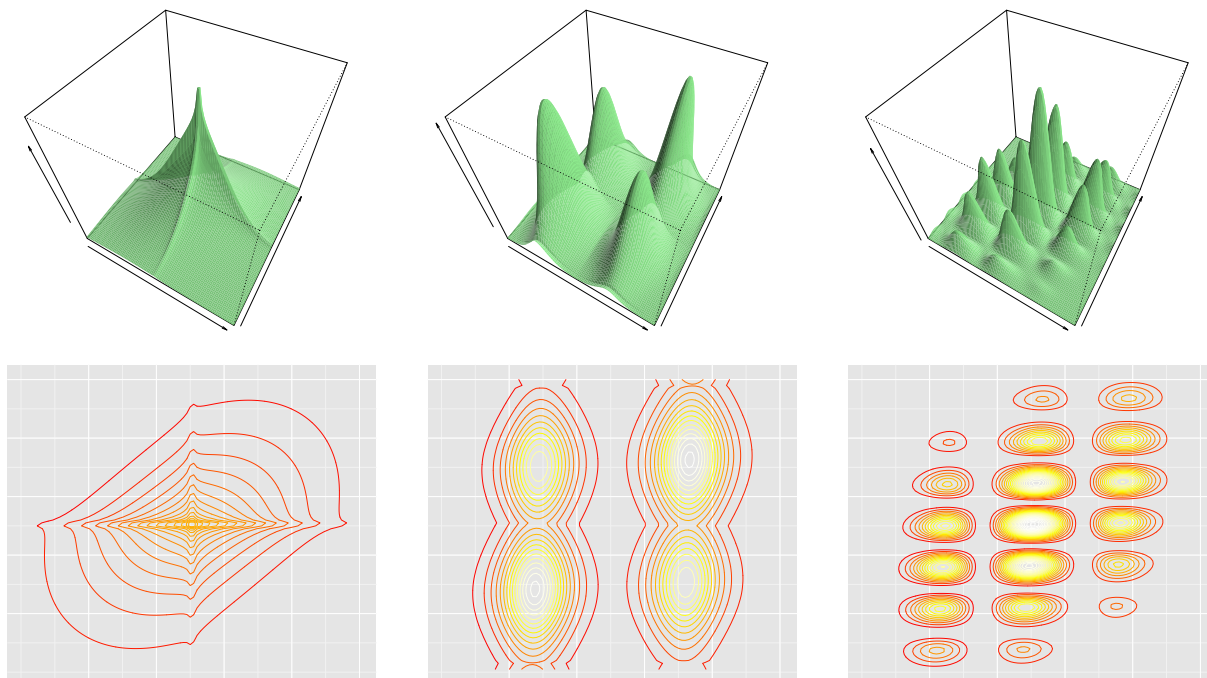


FIG. 3. Densities of three 2-dimensional nonparanormals. The left plots have component functions of the form $f_\alpha(x) = \text{sign}(x)|x|^\alpha$, with $\alpha_1 = 0.9$ and $\alpha_2 = 0.8$. The center plots have component functions of the form $g_\alpha(x) = \lfloor x \rfloor + 1/(1 + \exp(-\alpha(x - \lfloor x \rfloor - 1/2)))$ with $\alpha_1 = 10$ and $\alpha_2 = 5$, where $x - \lfloor x \rfloor$ is the fractional part. The right plots have component functions of the form $h_\alpha(x) = x + \sin(\alpha x)/\alpha$, with $\alpha_1 = 5$ and $\alpha_2 = 10$. In each case $\mu = (0, 0)$ and $\Sigma = \begin{pmatrix} 1 & 0.5 \\ 0.5 & 1 \end{pmatrix}$.

The assumption that $f(X) = (f_1(X_1), \dots, f_d(X_d))$ is Normal leads to a semiparametric model where only one-dimensional functions need to be estimated. But the monotonicity of the functions f_j , which map onto \mathbb{R} , enables computational tractability of the nonparanormal. For more general functions f , the normalizing constant for the density

$$p_X(x) \propto \exp\left\{-\frac{1}{2}(f(x) - \mu)^T \Sigma^{-1}(f(x) - \mu)\right\}$$

cannot be computed in closed form.

3.1 Connection to Copulae

If F_j is the distribution of X_j , then $U_j = F_j(X_j)$ is uniformly distributed on $(0, 1)$. Let C denote the joint distribution function of $U = (U_1, \dots, U_d)$, and let F denote the distribution function of X . Then we have that

$$\begin{aligned} (3.5) \quad F(x_1, \dots, x_d) &= \mathbb{P}(X_1 \leq x_1, \dots, X_d \leq x_d) \\ &= \mathbb{P}(F_1(X_1) \leq F_1(x_1), \dots, F_d(X_d) \leq F_d(x_d)) \end{aligned}$$

$$(3.6) \quad \leq F_1(x_1), \dots, F_d(x_d) \leq F_d(x_d)$$

$$(3.7) \quad = \mathbb{P}(U_1 \leq F_1(x_1), \dots, U_d \leq F_d(x_d))$$

$$(3.8) \quad = C(F_1(x_1), \dots, F_d(x_d)).$$

This is known as Sklar’s theorem (Sklar, 1959), and C is called a copula. If c is the density function of C , then

$$\begin{aligned} (3.9) \quad p(x_1, \dots, x_d) &= c(F_1(x_1), \dots, F_d(x_d)) \prod_{j=1}^d p(x_j), \end{aligned}$$

where $p(x_j)$ is the marginal density of X_j . For the nonparanormal we have

$$\begin{aligned} (3.10) \quad F(x_1, \dots, x_d) &= \Phi_{\mu, \Sigma}(\Phi^{-1}(F_1(x_1)), \dots, \Phi^{-1}(F_d(x_d))), \end{aligned}$$

where $\Phi_{\mu, \Sigma}$ is the multivariate Gaussian cdf, and Φ is the univariate standard Gaussian cdf.

The Gaussian copula is usually expressed in terms of the correlation matrix, which is given by $R = \text{diag}(\sigma)^{-1} \Sigma \text{diag}(\sigma)^{-1}$. Note that the univariate marginal density for a Normal can be written as $p(x_j) = \frac{1}{\sigma_j} \phi(u_j)$ where $u_j = (x_j - \mu_j)/\sigma_j$. The multivariate

Normal density can thus be expressed as

$$\begin{aligned}
 (3.11) \quad p_{\mu, \Sigma}(x_1, \dots, x_d) &= \frac{1}{(2\pi)^{d/2} |R|^{1/2} \prod_{j=1}^d \sigma_j} \\
 &\quad \cdot \exp\left(-\frac{1}{2} u^T R^{-1} u\right) \\
 (3.12) \quad &= \frac{1}{|R|^{1/2}} \exp\left(-\frac{1}{2} u^T (R^{-1} - I) u\right) \\
 &\quad \cdot \prod_{j=1}^d \frac{\phi(u_j)}{\sigma_j}.
 \end{aligned}$$

Since the distribution F_j of the j th variable satisfies $F_j(x_j) = \Phi((x_j - \mu_j)/\sigma_j) = \Phi(u_j)$, we have that $(X_j - \mu_j)/\sigma_j \stackrel{d}{=} \Phi^{-1}(F_j(X_j))$. The Gaussian copula density is thus

$$\begin{aligned}
 (3.13) \quad c(F_1(x_1), \dots, F_d(x_d)) &= \frac{1}{|R|^{1/2}} \exp\left\{-\frac{1}{2} \Phi^{-1}(F(x))^T \right. \\
 &\quad \left. \cdot (R^{-1} - I) \Phi^{-1}(F(x))\right\},
 \end{aligned}$$

where

$$\Phi^{-1}(F(x)) = (\Phi^{-1}(F_1(x_1)), \dots, \Phi^{-1}(F_d(x_d))).$$

This is seen to be equivalent to (3.1) using the chain rule and the identity

$$(3.14) \quad (\Phi^{-1})'(\eta) = \frac{1}{\phi(\Phi^{-1}(\eta))}.$$

3.2 Estimation

Let $X^{(1)}, \dots, X^{(n)}$ be a sample of size n where $X^{(i)} = (X_1^{(i)}, \dots, X_d^{(i)})^T \in \mathbb{R}^d$. We'll design a two-step estimation procedure where first the functions f_j are estimated, and then the inverse covariance matrix Ω is estimated, after transforming to approximately Normal.

In light of (3.4) we define

$$\hat{h}_j(x) = \Phi^{-1}(\tilde{F}_j(x)),$$

where \tilde{F}_j is an estimator of F_j . A natural candidate for \tilde{F}_j is the marginal empirical distribution function

$$\hat{F}_j(t) \equiv \frac{1}{n} \sum_{i=1}^n \mathbf{1}_{\{X_j^{(i)} \leq t\}}.$$

However, in this case $\hat{h}_j(x)$ blows up at the largest and smallest values of $X_j^{(i)}$. For the high-dimensional setting where n is small relative to d , an attractive alternative is to use a truncated or *Winsorized*² estimator,

$$(3.15) \quad \tilde{F}_j(x) = \begin{cases} \delta_n, & \text{if } \hat{F}_j(x) < \delta_n, \\ \hat{F}_j(x), & \text{if } \delta_n \leq \hat{F}_j(x) \leq 1 - \delta_n, \\ (1 - \delta_n), & \text{if } \hat{F}_j(x) > 1 - \delta_n, \end{cases}$$

where δ_n is a truncation parameter. There is a bias–variance tradeoff in choosing δ_n ; increasing δ_n increases the bias while it decreases the variance.

Given this estimate of the distribution of variable X_j , we then estimate the transformation function f_j by

$$(3.16) \quad \tilde{f}_j(x) \equiv \hat{\mu}_j + \hat{\sigma}_j \tilde{h}_j(x),$$

where

$$\tilde{h}_j(x) = \Phi^{-1}(\tilde{F}_j(x))$$

and $\hat{\mu}_j$ and $\hat{\sigma}_j$ are the sample mean and standard deviation.

$$\hat{\mu}_j \equiv \frac{1}{n} \sum_{i=1}^n X_j^{(i)} \quad \text{and} \quad \hat{\sigma}_j = \sqrt{\frac{1}{n} \sum_{i=1}^n (X_j^{(i)} - \hat{\mu}_j)^2}.$$

Now, let $S_n(\tilde{f})$ be the sample covariance matrix of $\tilde{f}(X^{(1)}), \dots, \tilde{f}(X^{(n)})$; that is,

$$\begin{aligned}
 (3.17) \quad S_n(\tilde{f}) &\equiv \frac{1}{n} \sum_{i=1}^n (\tilde{f}(X^{(i)}) - \mu_n(\tilde{f})) \\
 &\quad \cdot (\tilde{f}(X^{(i)}) - \mu_n(\tilde{f}))^T, \\
 \mu_n(\tilde{f}) &\equiv \frac{1}{n} \sum_{i=1}^n \tilde{f}(X^{(i)}).
 \end{aligned}$$

We then estimate Ω using $S_n(\tilde{f})$. For instance, the maximum likelihood estimator is $\hat{\Omega}_n^{\text{MLE}} = S_n(\tilde{f})^{-1}$.

The ℓ_1 -regularized estimator is

$$\begin{aligned}
 (3.18) \quad \hat{\Omega}_n &= \arg \min_{\Omega} \{ \text{tr}(\Omega S_n(\tilde{f})) \\
 &\quad - \log |\Omega| + \lambda \|\Omega\|_1 \},
 \end{aligned}$$

where λ is a regularization parameter, and $\|\Omega\|_1 = \sum_{j=1}^d \sum_{k=1}^d |\Omega_{jk}|$. The estimated graph is then $\hat{E}_n = \{(j, k) : \hat{\Omega}_{jk} \neq 0\}$.

Thus we use a two-step procedure to estimate the graph:

²After Charles P. Winsor, the statistician whom John Tukey credited with his conversion from topology to statistics (Mallows, 1990).

(1) Replace the observations, for each variable, by their respective Normal scores, subject to a Winsorized truncation.

(2) Apply the graphical lasso to the transformed data to estimate the undirected graph.

The first step is noniterative and computationally efficient. The truncation parameter δ_n is chosen to be

$$(3.19) \quad \delta_n = \frac{1}{4n^{1/4}\sqrt{\pi \log n}}$$

and does not need to be tuned. As will be shown in Theorem 3.1, such a choice makes the nonparanormal amenable to theoretical analysis.

3.3 Statistical Properties of $S_n(\tilde{f})$

The main technical result is an analysis of the covariance of the Winsorized estimator above. In particular, we show that under appropriate conditions,

$$\max_{j,k} |S_n(\tilde{f})_{jk} - S_n(f)_{jk}| = O_P\left(\sqrt{\frac{\log d + \log^2 n}{n^{1/2}}}\right),$$

where $S_n(\tilde{f})_{jk}$ denotes the (j, k) entry of the matrix $S_n(\tilde{f})$. This result allows us to leverage the significant body of theory on the graphical lasso (Rothman et al., 2008; Ravikumar et al., 2009) which we apply in step two.

THEOREM 3.1. *Suppose that $d = n^\xi$, and let \tilde{f} be the Winsorized estimator defined in (3.16) with $\delta_n = \frac{1}{4n^{1/4}\sqrt{\pi \log n}}$. Define*

$$C(M, \xi) \equiv \frac{48}{\sqrt{\pi \xi}}(\sqrt{2M} - 1)(M + 2)$$

for $M, \xi > 0$. Then for any $\varepsilon \geq C(M, \xi)\sqrt{\frac{\log d + \log^2 n}{n^{1/2}}}$ and sufficiently large n , we have

$$\begin{aligned} &\mathbb{P}\left(\max_{j,k} |S_n(\tilde{f})_{jk} - S_n(f)_{jk}| > \varepsilon\right) \\ &\leq \frac{c_1 d}{(n\varepsilon^2)^{2\xi}} + \frac{c_2 d}{n^{M\xi-1}} + c_3 \exp\left(-\frac{c_4 n^{1/2}\varepsilon^2}{\log d + \log^2 n}\right), \end{aligned}$$

where c_1, c_2, c_3, c_4 are positive constants.

The proof of this result involves a detailed Gaussian tail analysis, and is given in Liu, Lafferty and Wasserman (2009).

Using Theorem 3.1 and the results of Rothman et al. (2008), it can then be shown that the precision matrix is

estimated at the following rates in the Frobenius norm and the ℓ_2 -operator norm:

$$\|\widehat{\Omega}_n - \Omega_0\|_F = O_P\left(\sqrt{\frac{(s+d)\log d + \log^2 n}{n^{1/2}}}\right)$$

and

$$\|\widehat{\Omega}_n - \Omega_0\|_2 = O_P\left(\sqrt{\frac{s \log d + \log^2 n}{n^{1/2}}}\right),$$

where

$$s \equiv \text{Card}(\{(i, j) \in \{1, \dots, d\}\{1, \dots, d\} | \Omega_0(i, j) \neq 0, i \neq j\})$$

is the number of nonzero off-diagonal elements of the true precision matrix.

Using the results of Ravikumar et al. (2009), it can also be shown, under appropriate conditions, that the sparsity pattern of the precision matrix is estimated accurately with high probability. In particular, the nonparanormal estimator $\widehat{\Omega}_n$ satisfies

$$\mathbb{P}(\mathcal{G}(\widehat{\Omega}_n, \Omega_0)) \geq 1 - o(1),$$

where $\mathcal{G}(\widehat{\Omega}_n, \Omega_0)$ is the event

$$\{\text{sign}(\widehat{\Omega}_n(j, k)) = \text{sign}(\Omega_0(j, k)), \forall j, k \in \{1, \dots, d\}\}.$$

We refer to Liu, Lafferty and Wasserman (2009) for the details of the conditions and proofs. These $\tilde{O}_P(n^{-1/4})$ rates are slower than the $\tilde{O}_P(n^{-1/2})$ rates obtainable for the graphical lasso. However, in more recent work (Liu et al., 2012) we use estimators based on Spearman’s rho and Kendall’s tau statistics to obtain the parametric rate.

4. FOREST DENSITY ESTIMATION

We now describe a very different, but equally flexible and useful approach. Rather than assuming a transformation to normality and an arbitrary undirected graph, we restrict the graph to be a tree or forest, but allow arbitrary nonparametric distributions.

Let $p^*(x)$ be a probability density with respect to Lebesgue measure $\mu(\cdot)$ on \mathbb{R}^d , and let $X^{(1)}, \dots, X^{(n)}$ be n independent identically distributed \mathbb{R}^d -valued data vectors sampled from $p^*(x)$ where $X^{(i)} = (X_1^{(i)}, \dots, X_d^{(i)})$. Let \mathcal{X}_j denote the range of $X_j^{(i)}$, and let $\mathcal{X} = \mathcal{X}_1 \times \dots \times \mathcal{X}_d$.

A graph is a forest if it is acyclic. If F is a d -node undirected forest with vertex set $V_F = \{1, \dots, d\}$ and edge set $E_F \subset \{1, \dots, d\} \times \{1, \dots, d\}$, the number of

edges satisfies $|E_F| < d$. We say that a probability density function $p(x)$ is *supported by a forest* F if the density can be written as

$$(4.1) \quad p_F(x) = \prod_{(i,j) \in E_F} \frac{p(x_i, x_j)}{p(x_i)p(x_j)} \prod_{k \in V_F} p(x_k),$$

where each $p(x_i, x_j)$ is a bivariate density on $\mathcal{X}_i \times \mathcal{X}_j$, and each $p(x_k)$ is a univariate density on \mathcal{X}_k .

Let \mathcal{F}_d be the family of forests with d nodes, and let \mathcal{P}_d be the corresponding family of densities.

$$(4.2) \quad \mathcal{P}_d = \left\{ p \geq 0: \int_{\mathcal{X}} p(x) d\mu(x) = 1, \text{ and } p(x) \text{ satisfies (4.1) for some } F \in \mathcal{F}_d \right\}.$$

Define the oracle forest density

$$(4.3) \quad q^* = \arg \min_{q \in \mathcal{P}_d} D(p^* \| q)$$

where the Kullback–Leibler divergence $D(p \| q)$ between two densities p and q is

$$(4.4) \quad D(p \| q) = \int_{\mathcal{X}} p(x) \log \frac{p(x)}{q(x)} dx,$$

under the convention that $0 \log(0/q) = 0$, and $p \log(p/0) = \infty$ for $p \neq 0$. The following is straightforward to prove.

PROPOSITION 4.1. *Let q^* be defined as in (4.3). There exists a forest $F^* \in \mathcal{F}_d$, such that*

$$(4.5) \quad \begin{aligned} q^* &= p_{F^*}^* \\ &= \prod_{(i,j) \in E_{F^*}} \frac{p^*(x_i, x_j)}{p^*(x_i)p^*(x_j)} \prod_{k \in V_{F^*}} p^*(x_k), \end{aligned}$$

where $p^*(x_i, x_j)$ and $p^*(x_i)$ are the bivariate and univariate marginal densities of p^* .

For any density $q(x)$, the negative log-likelihood risk $R(q)$ is defined as

$$(4.6) \quad \begin{aligned} R(q) &= -\mathbb{E} \log q(X) \\ &= - \int_{\mathcal{X}} p^*(x) \log q(x) dx. \end{aligned}$$

It is straightforward to see that the density q^* defined in (4.3) also minimizes the negative log-likelihood loss.

$$(4.7) \quad \begin{aligned} q^* &= \arg \min_{q \in \mathcal{P}_d} D(p^* \| q) \\ &= \arg \min_{q \in \mathcal{P}_d} R(q). \end{aligned}$$

We thus define the oracle risk as $R^* = R(q^*)$. Using Proposition 4.1 and equation (4.1), we have

$$(4.8) \quad \begin{aligned} R^* &= R(q^*) = R(p_{F^*}^*) \\ &= - \int_{\mathcal{X}} p^*(x) \left(\sum_{(i,j) \in E_{F^*}} \log \frac{p^*(x_i, x_j)}{p^*(x_i)p^*(x_j)} + \sum_{k \in V_{F^*}} \log(p^*(x_k)) \right) dx \\ &= - \sum_{(i,j) \in E_{F^*}} I(X_i; X_j) + \sum_{k \in V_{F^*}} H(X_k), \end{aligned}$$

where

$$(4.9) \quad \begin{aligned} I(X_i; X_j) &= \int_{\mathcal{X}_i \times \mathcal{X}_j} p^*(x_i, x_j) \\ &\quad \cdot \log \frac{p^*(x_i, x_j)}{p^*(x_i)p^*(x_j)} dx_i dx_j \end{aligned}$$

is the mutual information between the pair of variables X_i, X_j , and

$$(4.10) \quad H(X_k) = - \int_{\mathcal{X}_k} p^*(x_k) \log p^*(x_k) dx_k$$

is the entropy.

4.1 A Two-Step Procedure

If the true density $p^*(x)$ were known, by Proposition 4.1, the density estimation problem would be reduced to finding the best forest structure F_d^* , satisfying

$$(4.11) \quad \begin{aligned} F_d^* &= \arg \min_{F \in \mathcal{F}_d} R(p_F^*) \\ &= \arg \min_{F \in \mathcal{F}_d} D(p^* \| p_F^*). \end{aligned}$$

The optimal forest F_d^* can be found by minimizing the right-hand side of (4.8). Since the entropy term $H(X) = \sum_k H(X_k)$ is constant across all forests, this can be recast as the problem of finding the maximum weight spanning forest for a weighted graph, where the weight of the edge connecting nodes i and j is $I(X_i; X_j)$. Kruskal’s algorithm (Kruskal, 1956) is a greedy algorithm that is guaranteed to find a maximum weight spanning tree of a weighted graph. In the setting of density estimation, this procedure was proposed by Chow and Liu (1968) as a way of constructing a tree approximation to a distribution. At each stage the algorithm adds an edge connecting that pair of variables with maximum mutual information among all pairs not yet visited by the algorithm, if doing so does not form a cycle. When stopped early, after $k < d - 1$ edges have been added, it yields the best k -edge weighted forest.

Of course, the above procedure is not practical since the true density $p^*(x)$ is unknown. We replace the population mutual information $I(X_i; X_j)$ in (4.8) by a plug-in estimate $\widehat{I}_n(X_i; X_j)$, defined as

$$(4.12) \quad \widehat{I}_n(X_i; X_j) = \int_{\mathcal{X}_i \times \mathcal{X}_j} \widehat{p}_n(x_i, x_j) \cdot \log \frac{\widehat{p}_n(x_i, x_j)}{\widehat{p}_n(x_i) \widehat{p}_n(x_j)} dx_i dx_j,$$

where $\widehat{p}_n(x_i, x_j)$ and $\widehat{p}_n(x_i)$ are bivariate and univariate kernel density estimates. Given this estimated mutual information matrix $\widehat{M}_n = [\widehat{I}_n(X_i; X_j)]$, we can then apply Kruskal’s algorithm (equivalently, the Chow–Liu algorithm) to find the best tree structure \widehat{F}_n .

Since the number of edges of \widehat{F}_n controls the number of degrees of freedom in the final density estimator, an automatic data-dependent way to choose it is needed. We adopt the following two-stage procedure. First, we randomly split the data into two sets \mathcal{D}_1 and \mathcal{D}_2 of sizes n_1 and n_2 ; we then apply the following steps:

(1) Using \mathcal{D}_1 , construct kernel density estimates of the univariate and bivariate marginals and calculate $\widehat{I}_{n_1}(X_i; X_j)$ for $i, j \in \{1, \dots, d\}$ with $i \neq j$. Construct a full tree $\widehat{F}_{n_1}^{(d-1)}$ with $d - 1$ edges, using the Chow–Liu algorithm.

(2) Using \mathcal{D}_2 , prune the tree $\widehat{F}_{n_1}^{(d-1)}$ to find a forest $\widehat{F}_{n_1}^{(\widehat{k})}$ with \widehat{k} edges, for $0 \leq \widehat{k} \leq d - 1$.

Once $\widehat{F}_{n_1}^{(\widehat{k})}$ is obtained in Step 2, we can calculate $\widehat{p}_{\widehat{F}_{n_1}^{(\widehat{k})}}$ according to (4.1), using the kernel density estimates constructed in Step 1.

4.1.1 Step 1: Constructing a sequence of forests. Step 1 is carried out on the dataset \mathcal{D}_1 . Let $K(\cdot)$ be a univariate kernel function. Given an evaluation point (x_i, x_j) , the bivariate kernel density estimate for (X_i, X_j) based on the observations $\{X_i^{(s)}, X_j^{(s)}\}_{s \in \mathcal{D}_1}$ is defined as

$$(4.13) \quad \widehat{p}_{n_1}(x_i, x_j) = \frac{1}{n_1} \sum_{s \in \mathcal{D}_1} \frac{1}{h_2^2} K\left(\frac{X_i^{(s)} - x_i}{h_2}\right) K\left(\frac{X_j^{(s)} - x_j}{h_2}\right),$$

where we use a product kernel with $h_2 > 0$ as the bandwidth parameter. The univariate kernel density estimate $\widehat{p}_{n_1}(x_k)$ for X_k is

$$(4.14) \quad \widehat{p}_{n_1}(x_k) = \frac{1}{n_1} \sum_{s \in \mathcal{D}_1} \frac{1}{h_1} K\left(\frac{X_k^{(s)} - x_k}{h_1}\right),$$

where $h_1 > 0$ is the univariate bandwidth.

We assume that the data lie in a d -dimensional unit cube $\mathcal{X} = [0, 1]^d$. To calculate the empirical mutual information $\widehat{I}_{n_1}(X_i; X_j)$, we need to numerically evaluate a two-dimensional integral. To do so, we calculate the kernel density estimates on a grid of points. We choose m evaluation points on each dimension, $x_{1i} < x_{2i} < \dots < x_{mi}$ for the i th variable. The mutual information $\widehat{I}_{n_1}(X_i; X_j)$ is then approximated as

$$(4.15) \quad \widehat{I}_{n_1}(X_i; X_j) = \frac{1}{m^2} \sum_{k=1}^m \sum_{\ell=1}^m \widehat{p}_{n_1}(x_{ki}, x_{\ell j}) \cdot \log \frac{\widehat{p}_{n_1}(x_{ki}, x_{\ell j})}{\widehat{p}_{n_1}(x_{ki}) \widehat{p}_{n_1}(x_{\ell j})}.$$

The approximation error can be made arbitrarily small by choosing m sufficiently large. As a practical concern, care needs to be taken that the factors $\widehat{p}_{n_1}(x_{ki})$ and $\widehat{p}_{n_1}(x_{\ell j})$ in the denominator are not too small; a truncation procedure can be used to ensure this. Once the $d \times d$ mutual information matrix $\widehat{M}_{n_1} = [\widehat{I}_{n_1}(X_i; X_j)]$ is obtained, we can apply the Chow–Liu (Kruskal) algorithm to find a maximum weight spanning tree (see Algorithm 1).

4.1.2 Step 2: Selecting a forest size. The full tree $\widehat{F}_{n_1}^{(d-1)}$ obtained in Step 1 might have high variance when the dimension d is large, leading to overfitting in the density estimate. In order to reduce the variance, we prune the tree; that is, we choose an unconnected tree with k edges. The number of edges k is a tuning parameter that induces a bias–variance tradeoff.

In order to choose k , note that in stage k of the Chow–Liu algorithm, we have an edge set $E^{(k)}$ (in the notation of the Algorithm 1) which corresponds to a forest $\widehat{F}_{n_1}^{(k)}$ with k edges, where $F_{n_1}^{(0)}$ is the union of d disconnected nodes. To select k , we cross-validate over the d forests $\widehat{F}_{n_1}^{(0)}, \widehat{F}_{n_1}^{(1)}, \dots, \widehat{F}_{n_1}^{(d-1)}$.

Algorithm 1 Tree construction (Kruskal/Chow–Liu)

Input: Data set \mathcal{D}_1 and the bandwidths h_1, h_2 .

Initialize: Calculate \widehat{M}_{n_1} , according to (4.13), (4.14) and (4.15).

Set $E^{(0)} = \emptyset$.

For $k = 1, \dots, d - 1$:

(1) Set $(i^{(k)}, j^{(k)}) \leftarrow \arg \max_{(i,j)} \widehat{M}_{n_1}(i, j)$ such that $E^{(k-1)} \cup \{(i^{(k)}, j^{(k)})\}$ does not contain a cycle;

(2) $E^{(k)} \leftarrow E^{(k-1)} \cup \{(i^{(k)}, j^{(k)})\}$.

Output: tree $\widehat{F}_{n_1}^{(d-1)}$ with edge set $E^{(d-1)}$.

Let $\widehat{p}_{n_2}(x_i, x_j)$ and $\widehat{p}_{n_2}(x_k)$ be defined as in (4.13) and (4.14), but now evaluated solely based on the held-out data in \mathcal{D}_2 . For a density p_F that is supported by a forest F , we define the held-out negative log-likelihood risk as

$$\begin{aligned} & \widehat{R}_{n_2}(p_F) \\ &= - \sum_{(i,j) \in E_F} \int_{\mathcal{X}_i \times \mathcal{X}_j} \widehat{p}_{n_2}(x_i, x_j) \\ & \quad \cdot \log \frac{p(x_i, x_j)}{p(x_i)p(x_j)} dx_i dx_j \\ & \quad - \sum_{k \in V_F} \int_{\mathcal{X}_k} \widehat{p}_{n_2}(x_k) \log p(x_k) dx_k. \end{aligned} \tag{4.16}$$

The selected forest is then $\widehat{F}_{n_1}^{(\widehat{k})}$ where

$$\widehat{k} = \arg \min_{k \in \{0, \dots, d-1\}} \widehat{R}_{n_2}(\widehat{p}_{F_{n_1}^{(k)}}) \tag{4.17}$$

and where $\widehat{p}_{F_{n_1}^{(k)}}$ is computed using the density estimate \widehat{p}_{n_1} constructed on \mathcal{D}_1 .

We can also estimate \widehat{k} as

$$\begin{aligned} & \widehat{k} = \arg \max_{k \in \{0, \dots, d-1\}} \frac{1}{n_2} \\ & \quad \cdot \sum_{s \in \mathcal{D}_2} \log \left(\prod_{(i,j) \in E_{F^{(k)}}} \frac{\widehat{p}_{n_1}(X_i^{(s)}, X_j^{(s)})}{\widehat{p}_{n_1}(X_i^{(s)})\widehat{p}_{n_1}(X_j^{(s)})} \right. \\ & \quad \quad \left. \cdot \prod_{\ell \in V_{F^{(k)}}} \widehat{p}_{n_1}(X_\ell^{(s)}) \right) \\ &= \arg \max_{k \in \{0, \dots, d-1\}} \frac{1}{n_2} \end{aligned} \tag{4.18}$$

$$\cdot \sum_{s \in \mathcal{D}_2} \log \left(\prod_{(i,j) \in E_{F^{(k)}}} \frac{\widehat{p}_{n_1}(X_i^{(s)}, X_j^{(s)})}{\widehat{p}_{n_1}(X_i^{(s)})\widehat{p}_{n_1}(X_j^{(s)})} \right). \tag{4.19}$$

This minimization can be efficiently carried out by iterating over the $d - 1$ edges in $\widehat{F}_{n_1}^{(d-1)}$.

Once \widehat{k} is obtained, the final forest-based kernel density estimate is given by

$$\widehat{p}_n(x) = \prod_{(i,j) \in E(\widehat{k})} \frac{\widehat{p}_{n_1}(x_i, x_j)}{\widehat{p}_{n_1}(x_i)\widehat{p}_{n_1}(x_j)} \prod_k \widehat{p}_{n_1}(x_k). \tag{4.20}$$

Another alternative is to compute a maximum weight spanning forest, using Kruskal’s algorithm, but with held-out edge weights

$$\widehat{w}_{n_2}(i, j) = \frac{1}{n_2} \sum_{s \in \mathcal{D}_2} \log \frac{\widehat{p}_{n_1}(X_i^{(s)}, X_j^{(s)})}{\widehat{p}_{n_1}(X_i^{(s)})\widehat{p}_{n_1}(X_j^{(s)})}. \tag{4.21}$$

In fact, asymptotically (as $n_2 \rightarrow \infty$) this gives an optimal tree-based estimator constructed in terms of the kernel density estimates \widehat{p}_{n_1} .

4.2 Statistical Properties

The statistical properties of the forest density estimator can be analyzed under the same type of assumptions that are made for classical kernel density estimation. In particular, assume that the univariate and bivariate densities lie in a Hölder class with exponent β . Under this assumption the minimax rate of convergence in the squared error loss is $O(n^{\beta/(\beta+1)})$ for bivariate densities and $O(n^{2\beta/(2\beta+1)})$ for univariate densities. Technical assumptions on the kernel yield L_∞ concentration results on kernel density estimation (Giné and Guillou, 2002).

Choose the bandwidths h_1 and h_2 to be used in the one-dimensional and two-dimensional kernel density estimates according to

$$h_1 \asymp \left(\frac{\log n}{n} \right)^{1/(1+2\beta)}, \tag{4.22}$$

$$h_2 \asymp \left(\frac{\log n}{n} \right)^{1/(2+2\beta)}. \tag{4.23}$$

This choice of bandwidths ensures the optimal rate of convergence. Let $\mathcal{P}_d^{(k)}$ be the family of d -dimensional densities that are supported by forests with at most k edges. Then

$$\mathcal{P}_d^{(0)} \subset \mathcal{P}_d^{(1)} \subset \dots \subset \mathcal{P}_d^{(d-1)}. \tag{4.24}$$

Due to this nesting property,

$$\begin{aligned} \inf_{q_F \in \mathcal{P}_d^{(0)}} R(q_F) &\geq \inf_{q_F \in \mathcal{P}_d^{(1)}} R(q_F) \\ &\geq \dots \geq \inf_{q_F \in \mathcal{P}_d^{(d-1)}} R(q_F). \end{aligned} \tag{4.25}$$

This means that a full spanning tree would generally be selected if we had access to the true distribution. However, with access to finite data to estimate the densities (\widehat{p}_{n_1}), the optimal procedure is to use fewer than $d - 1$ edges. The following result analyzes the excess risk resulting from selecting the forest based on the heldout risk \widehat{R}_{n_2} .

THEOREM 4.1. *Let $\widehat{p}_{\widehat{F}_d^{(k)}}$ be the estimate with $|E_{\widehat{F}_d^{(k)}}| = k$ obtained after the first k iterations of the Chow–Liu algorithm. Then under (omitted) technical assumptions on the densities and kernel, for any*

$1 \leq k \leq d-1$,

$$(4.26) \quad \begin{aligned} & R(\widehat{p}_{\widehat{F}_d^{(k)}}) - \inf_{q_F \in \mathcal{P}_d^{(k)}} R(q_F) \\ &= O_P \left(k \sqrt{\frac{\log n + \log d}{n^{\beta/(1+\beta)}}} + d \sqrt{\frac{\log n + \log d}{n^{2\beta/(1+2\beta)}}} \right) \end{aligned}$$

and

$$(4.27) \quad \begin{aligned} & R(\widehat{p}_{\widehat{F}_d^{(\widehat{k})}}) - \min_{0 \leq k \leq d-1} R(\widehat{p}_{\widehat{F}_d^{(k)}}) \\ &= O_P \left((k^* + \widehat{k}) \sqrt{\frac{\log n + \log d}{n^{\beta/(1+\beta)}}} \right. \\ & \quad \left. + d \sqrt{\frac{\log n + \log d}{n^{2\beta/(1+2\beta)}}} \right), \end{aligned}$$

where $\widehat{k} = \arg \min_{0 \leq k \leq d-1} \widehat{R}_{n_2}(\widehat{p}_{\widehat{F}_d^{(k)}})$ and $k^* = \arg \min_{0 \leq k \leq d-1} R(\widehat{p}_{\widehat{F}_d^{(k)}})$.

The main work in proving this result lies in establishing bounds such as

$$(4.28) \quad \begin{aligned} & \sup_{F \in \mathcal{F}_d^{(k)}} |R(\widehat{p}_F) - \widehat{R}_{n_2}(\widehat{p}_F)| \\ &= O_P(\phi_n(k) + \psi_n(d)), \end{aligned}$$

where \widehat{R}_{n_2} is the held-out risk, under the notation

$$(4.29) \quad \phi_n(k) = k \sqrt{\frac{\log n + \log d}{n^{\beta/(\beta+1)}}},$$

$$(4.30) \quad \psi_n(d) = d \sqrt{\frac{\log n + \log d}{n^{2\beta/(1+2\beta)}}}.$$

For the proof of this and related results, see Liu et al. (2011). Using this, one easily obtains

$$(4.31) \quad \begin{aligned} & R(\widehat{p}_{\widehat{F}_d^{(\widehat{k})}}) - R(\widehat{p}_{\widehat{F}_d^{(k^*)}}) \\ &= R(\widehat{p}_{\widehat{F}_d^{(\widehat{k})}}) - \widehat{R}_{n_2}(\widehat{p}_{\widehat{F}_d^{(\widehat{k})}}) \\ & \quad + \widehat{R}_{n_2}(\widehat{p}_{\widehat{F}_d^{(\widehat{k})}}) - R(\widehat{p}_{\widehat{F}_d^{(k^*)}}) \end{aligned}$$

$$(4.32) \quad \begin{aligned} &= O_P(\phi_n(\widehat{k}) + \psi_n(d)) \\ & \quad + \widehat{R}_{n_2}(\widehat{p}_{\widehat{F}_d^{(\widehat{k})}}) - R(\widehat{p}_{\widehat{F}_d^{(k^*)}}) \end{aligned}$$

$$(4.33) \quad \begin{aligned} &\leq O_P(\phi_n(\widehat{k}) + \psi_n(d)) \\ & \quad + \widehat{R}_{n_2}(\widehat{p}_{\widehat{F}_d^{(k^*)}}) - R(\widehat{p}_{\widehat{F}_d^{(k^*)}}) \end{aligned}$$

$$(4.34) \quad = O_P(\phi_n(\widehat{k}) + \phi_n(k^*) + \psi_n(d)),$$

where (4.33) follows from the fact that \widehat{k} is the minimizer of $\widehat{R}_{n_2}(\cdot)$. This result allows the dimension d to increase at a rate $o(\sqrt{n^{2\beta/(1+2\beta)}/\log n})$, and the number of edges k to increase at a rate $o(\sqrt{n^{\beta/(1+\beta)}/\log n})$, with the excess risk still decreasing to zero asymptotically.

Note that the minimax rate for 2-dimensional kernel density estimation under our stated conditions is $n^{-\beta/(\beta+1)}$. The rate above is essentially the square root of this rate, up to logarithmic factors. This is because a higher order kernel is used, which may result in negative values. Once we correct these negative values, the resulting estimated density will no longer integrate to one. The slower rate is due to a very simple truncation technique to correct the higher-order kernel density estimator to estimate mutual information. Current work is investigating a different version of the higher order kernel density estimator with more careful correction techniques, for which it is possible to achieve the optimal minimax rate.

In theory the bandwidths are chosen as in (4.22) and (4.23), assuming β is known. In our experiments presented below, the bandwidth h_k for the 2-dimensional kernel density estimator is chosen according to the Normal reference rule

$$(4.35) \quad \begin{aligned} h_k &= 1.06 \cdot \min \left\{ \widehat{\sigma}_k, \frac{\widehat{q}_{k,0.75} - \widehat{q}_{k,0.25}}{1.34} \right\} \\ &\quad \cdot n^{-1/(2\beta+2)}, \end{aligned}$$

where $\widehat{\sigma}_k$ is the sample standard deviation of $\{X_k^{(s)}\}_{s \in \mathcal{D}_1}$, and $\widehat{q}_{k,0.75}$, $\widehat{q}_{k,0.25}$ are the 75% and 25% sample quantiles of $\{X_k^{(s)}\}_{s \in \mathcal{D}_1}$, with $\beta = 2$. See Wasserman (2006) for a discussion of this choice of bandwidth.

5. EXAMPLES

5.1 Gene–Gene Interaction Graphs

The nonparanormal and Gaussian graphical model can construct very different graphs. Here we consider a data set based on Affymetrix GeneChip microarrays for the plant *Arabidopsis thaliana* (Wille et al., 2004) (see Figure 4). The sample size is $n = 118$. The expression levels for each chip are pre-processed by log-transformation and standardization. A subset of 40 genes from the isoprenoid pathway is chosen for analysis.

While these data are often treated as multivariate Gaussian, the nonparanormal and the glasso give very



source: wikipedia.org

FIG. 4. *Arabidopsis thaliana* is a small flowering plant; it was the first plant genome to be sequenced, and its roughly 27,000 genes and 35,000 proteins have been actively studied. Here we consider a data set based on Affymetrix GeneChip microarrays with sample size $n = 118$, for which $d = 40$ genes have been selected for analysis.

different graphs over a wide range of regularization parameters, suggesting that the nonparametric method could lead to different biological conclusions.

The regularization paths of the two methods are compared in Figure 5. To generate the paths, we select 50 regularization parameters on an evenly spaced grid in the interval $[0.16, 1.2]$. Although the paths for the two methods look similar, there are some subtle dif-

ferences. In particular, variables become nonzero in a different order.

Figure 6 compares the estimated graphs for the two methods at several values of the regularization parameter λ in the range $[0.16, 0.37]$. For each λ , we show the estimated graph from the nonparanormal in the first column. In the second column we show the graph obtained by scanning the full regularization path of the glasso fit and finding the graph having the smallest symmetric difference with the nonparanormal graph. The symmetric difference graph is shown in the third column. The closest glasso fit is different, with edges selected by the glasso not selected by the nonparanormal, and vice-versa. The estimated transformation functions for several genes are shown Figure 7, which show non-Gaussian behavior.

Since the graphical lasso typically results in a large parameter bias as a consequence of the ℓ_1 regularization, it sometimes make sense to use the *refit glasso*, which is a two-step procedure—in the first step, a sparse inverse covariance matrix is obtained by the graphical lasso; in the second step, a Gaussian model is refit without ℓ_1 regularization, but enforcing the sparsity pattern obtained in the first step.

Figure 8 compares forest density estimation to the graphical lasso and refit glasso. It can be seen that the forest-based kernel density estimator has better generalization performance. This is not surprising, given that the true distribution of the data is not Gaussian. (Note that since we do not directly compute the marginal univariate densities in the nonparanormal, we are unable to compute likelihoods under this model.) The held-out log-likelihood curve for forest density estimation

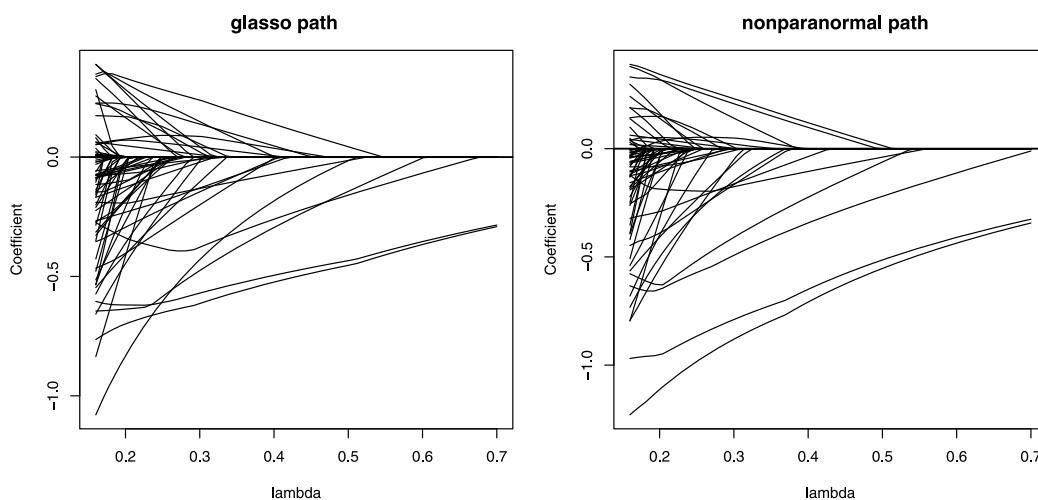


FIG. 5. Regularization paths of both methods on the microarray data set. Although the paths for the two methods look similar, there are some subtle differences.

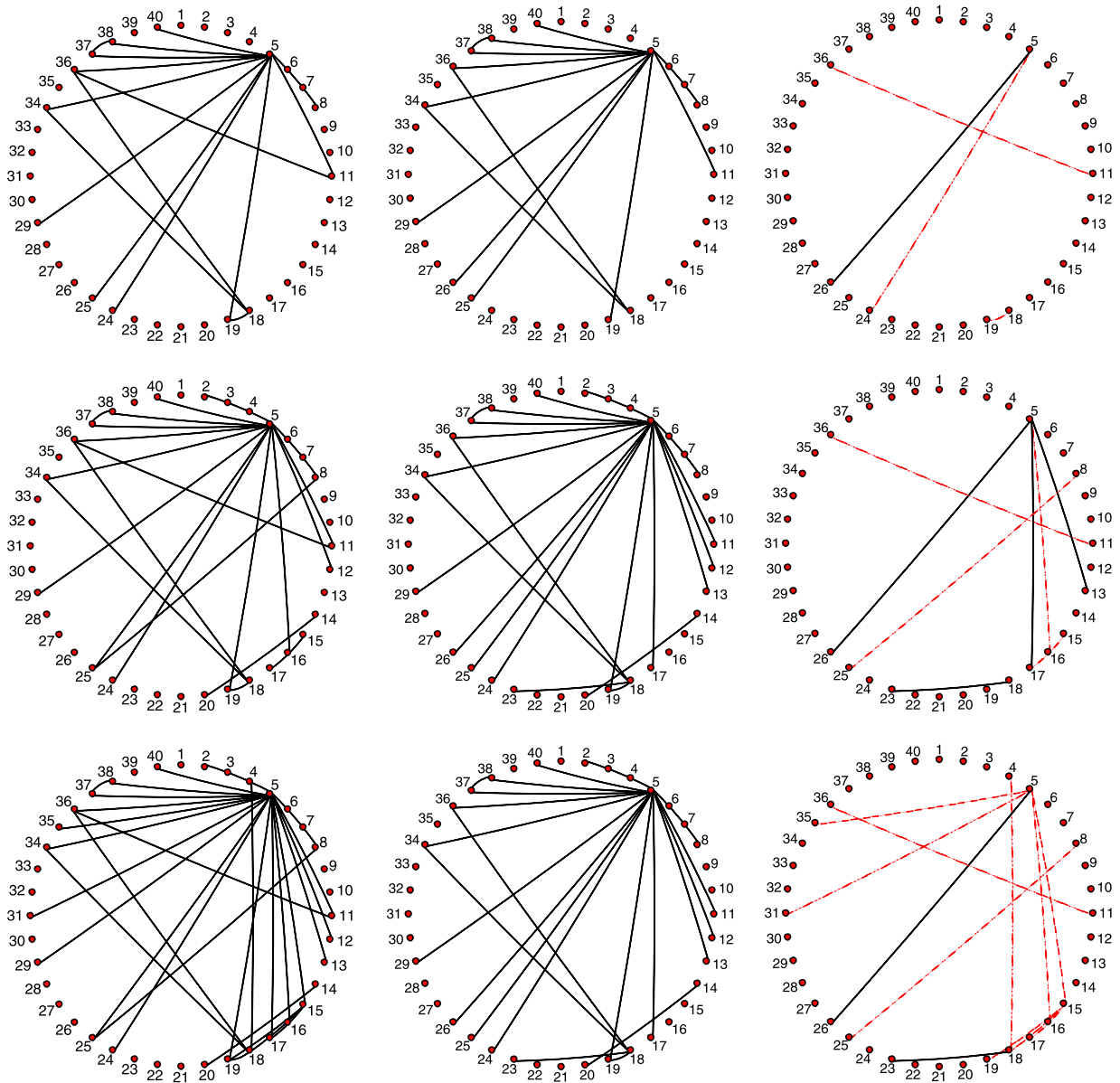


FIG. 6. The nonparanormal estimated graph for three values of $\lambda = 0.2448, 0.2661, 0.30857$ (left column), the closest glasso estimated graph from the full path (middle) and the symmetric difference graph (right).

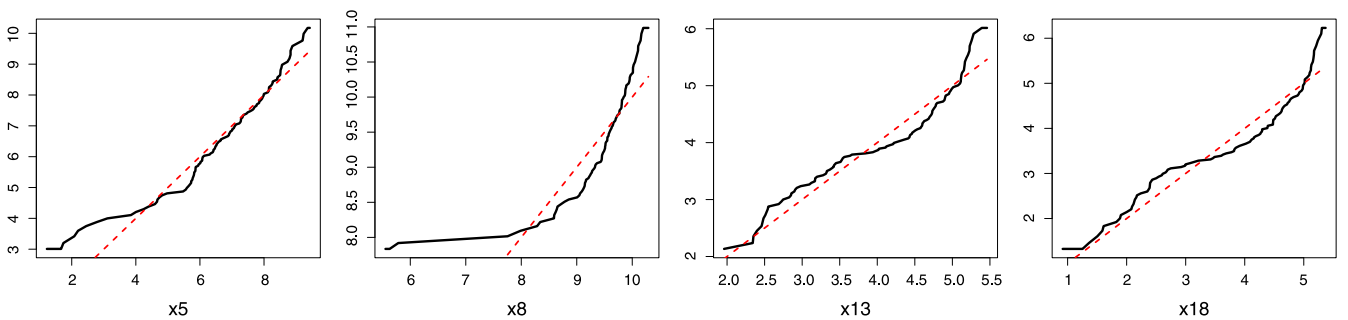


FIG. 7. Estimated transformation functions for four genes in the microarray data set, indicating non-Gaussian marginals. The corresponding genes are among the nodes appearing in the symmetric difference graphs above.

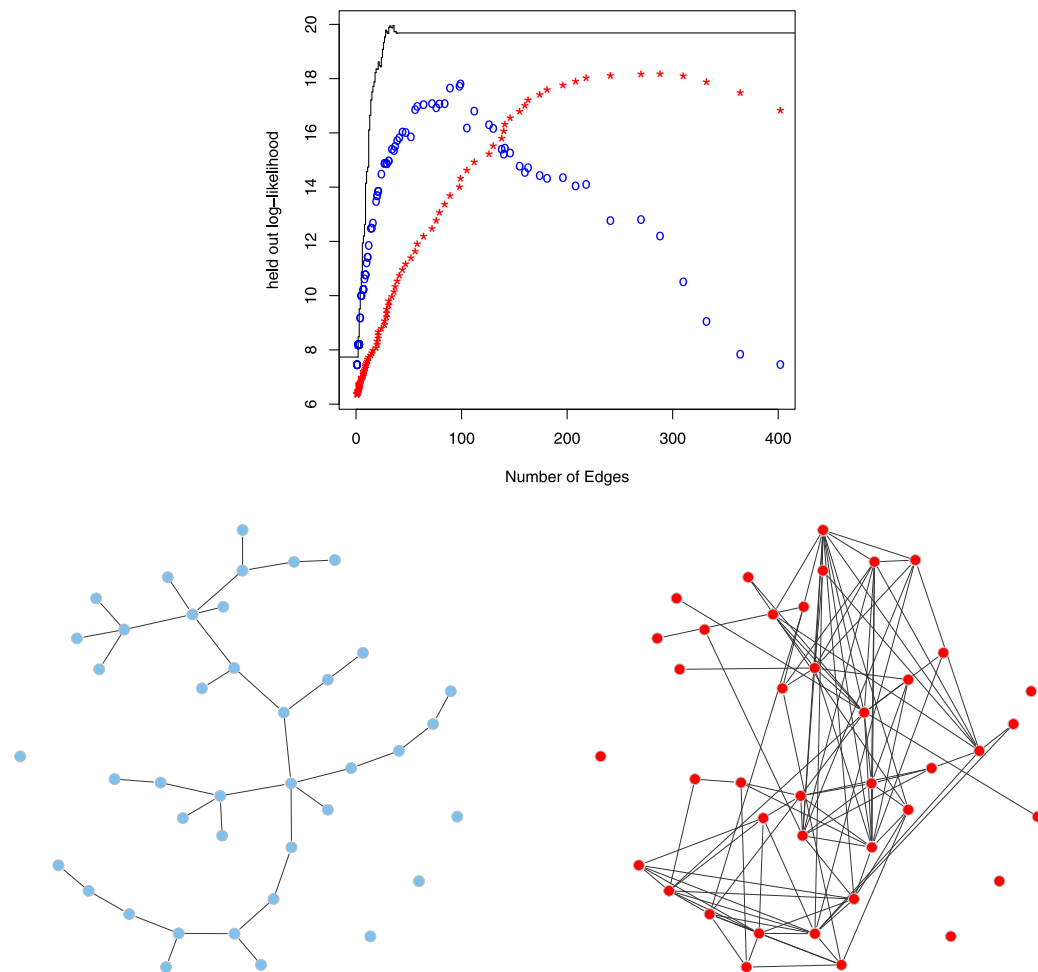


FIG. 8. Results on microarray data. Top: held-out log-likelihood of the forest density estimator (black step function), glasso (red stars) and refit glasso (blue circles). Bottom: estimated graphs using the forest-based estimator (left) and the glasso (right), using the same node layout.

achieves a maximum when there are only 35 edges in the model. In contrast, the held-out log-likelihood curves of the glasso and refit glasso achieve maxima when there are around 280 edges and 100 edges respectively, while their predictive estimates are still inferior to those of the forest-based kernel density estimator. Figure 8 also shows the estimated graphs for the forest-based kernel density estimator and the graphical lasso. The graphs are automatically selected based on held-out log-likelihood, and are clearly different.

5.2 Graphs for Equities Data

For the examples in this section we collected stock price data from Yahoo! Finance (finance.yahoo.com). The daily closing prices were obtained for 452 stocks that consistently were in the S&P 500 index between January 1, 2003 through January 1, 2011. This gave us altogether 2015 data points, each data point corresponds to the vector of closing prices on a trading day.

With $S_{t,j}$ denoting the closing price of stock j on day t , we consider the variables $X_{tj} = \log(S_{t,j}/S_{t-1,j})$ and build graphs over the indices j . We simply treat the instances X_t as independent replicates, even though they form a time series. The data contain many outliers; the reasons for these outliers include splits in a stock, which increases the number of shares. We Winsorize (or truncate) every stock so that its data points are within three times the mean absolute deviation from the sample average. The importance of this Winsorization is shown below; see the “snake graph” in Figure 10. For the following results we use the subset of the data between January 1, 2003 to January 1, 2008, before the onset of the “financial crisis.” It is interesting to compare to results that include data after 2008, but we omit these for brevity.

The 452 stocks are categorized into 10 Global Industry Classification Standard (GICS) sectors, including

Target Corp.	(Consumer Discr.)		
Big Lots, Inc.	(Consumer Discr.)		
Costco Co.	(Consumer Staples)		
Family Dollar Stores	(Consumer Discr.)		
Kohl's Corp.	(Consumer Discr.)		
Lowe's Cos.	(Consumer Discr.)		
Macy's Inc.	(Consumer Discr.)		
Wal-Mart Stores	(Consumer Staples)		
		Yahoo Inc.	(Information Tech.)
		Amazon.com Inc.	(Consumer Discr.)
		eBay Inc.	(Information Tech.)
		NetApp	(Information Tech.)

FIG. 9. Example neighborhoods in a forest graph for two stocks, Yahoo Inc. and Target Corp. The corresponding GICS industries are shown in parentheses. (Consumer Discr. is short for Consumer Discretionary, and Information Tech. is short for Information Technology.)

Consumer Discretionary (70 stocks), Consumer Staples (35 stocks), Energy (37 stocks), Financials (74 stocks), Health Care (46 stocks), Industrials (59 stocks), Information Technology (64 stocks), Materials (29 stocks), Telecommunications Services (6 stocks), and Utilities (32 stocks). In the graphs shown below, the nodes are colored according to the GICS sector of the corresponding stock. It is expected that stocks from the same GICS sectors should tend to be clustered together, since stocks from the same GICS sector tend to interact more with each other. This is indeed this case; for example, Figure 9 shows examples of the neighbors of two stocks, Yahoo Inc. and Target Corp., in the forest density graph.

Figures 10(a)–(c) show graphs estimated using the glasso, nonparanormal, and forest density estimator on the data from January 1, 2003 to January 1, 2008. There are altogether $n = 1257$ data points and $d = 452$ dimensions. To estimate the glasso graph, we somewhat arbitrarily set the regularization parameter to $\lambda = 0.55$, which results in a graph that has 1316 edges, about 3 neighbors per node, and good clustering structure. The resulting graph is shown in Figure 10(a). The corresponding nonparanormal graph is shown in Figure 10(b). The regularization is chosen so that it too has 1316 edges. Only nodes that have neighbors in one of the graphs are shown; the remaining nodes are disconnected.

Since our dataset contains $n = 1257$ data points, we directly apply the forest density estimator on the whole dataset to obtain a full spanning tree of $d - 1 = 451$ edges. This estimator turns out to be very sensitive to outliers, since it exploits kernel density estimates as building blocks. In Figure 10(d) we show the estimated forest density graph on the stock data when outliers are *not* trimmed by Winsorization. In this case

the graph is anomalous, with a snake-like character that weaves in and out of the 10 GICS industries. Intuitively, the outliers make the two-dimensional densities appear like thin “pancakes,” and densities with similar orientations are clustered together. To address this, we trim the outliers by Winsorizing at 3 MADs, as described above. Figure 10(c) shows the estimated forest graph, restricted to the same stocks shown for the graphs in (a) and (b). The resulting graph has good clustering with respect to the GICS sectors.

Figures 11(a)–(c) display the differences and edges common to the glasso, nonparanormal and forest graphs. Figure 11(a) shows the symmetric difference between the estimated glasso and nonparanormal graphs, and Figure 11(b) shows the common edges. Figure 11(c) shows the symmetric difference between the nonparanormal and forest graphs, and Figure 11(d) shows the common edges.

We refrain from drawing any hard conclusions about the effectiveness of the different methods based on these plots—how these graphs are used will depend on the application. These results serve mainly to highlight how very different inferences about the independence relations can arise from moving from a Gaussian model to a semiparametric model to a fully nonparametric model with restricted graphs.

6. RELATED WORK

There is surprisingly little work on structure learning of nonparametric graphical models in high dimensions. One piece of related work is sparse log-density smoothing spline ANOVA models, introduced by Jeon and Lin (2006). In such a model the log-density function is decomposed as the sum of a constant term, one-dimensional functions (main effects), two-dimensional

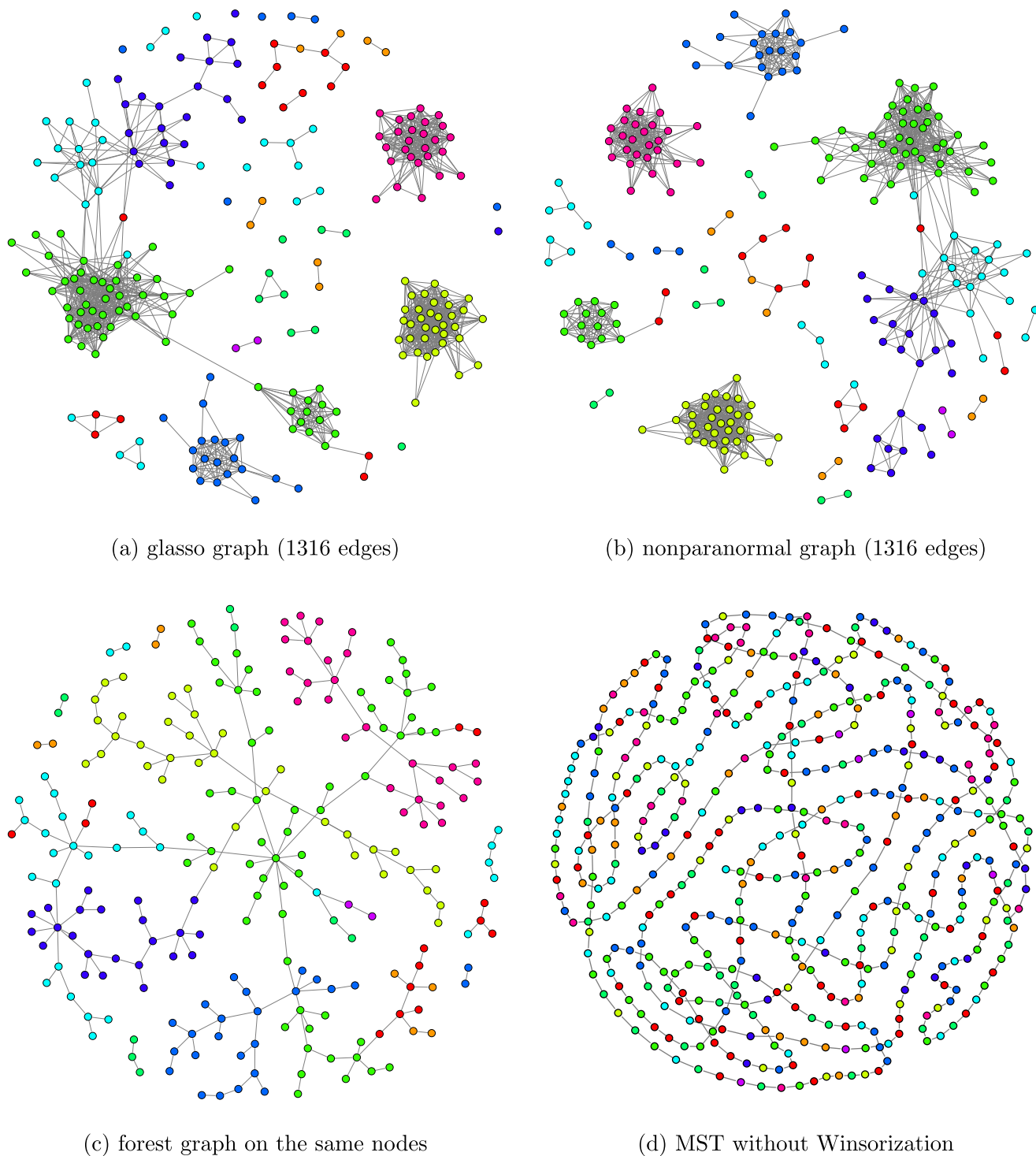


FIG. 10. Graphs build on S&P 500 stock data from Jan. 1, 2003 to Jan. 1, 2008. The graphs are estimated using (a) the glasso, (b) the nonparanormal and (c) forest density estimation. The nodes are colored according to their GICS sector categories. Nodes are not shown that have zero neighbors in both the glasso and nonparanormal graphs. Figure (d) shows the maximum weight spanning tree that results if the data are not Winsorized to trim outliers.

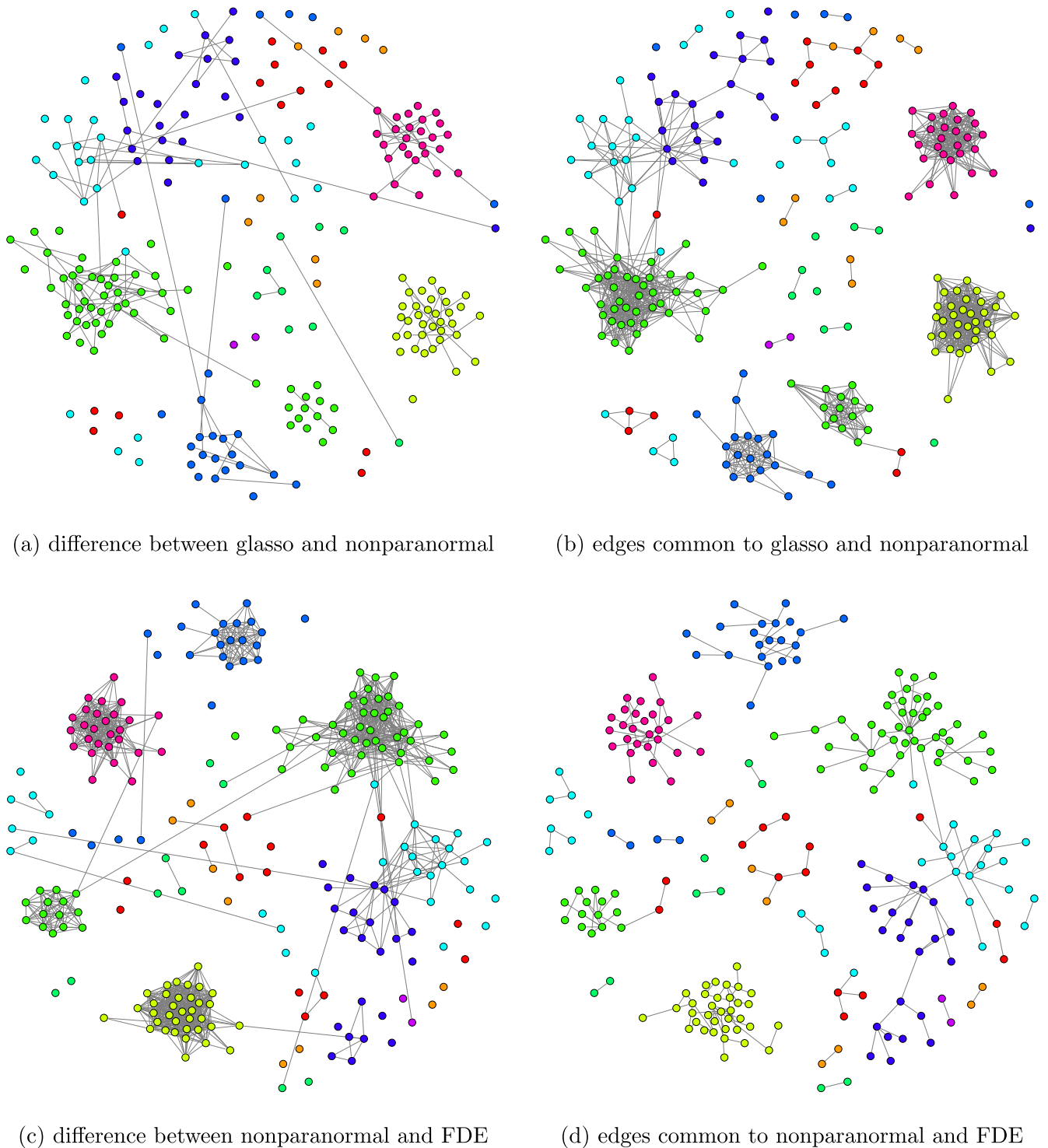


FIG. 11. Visualizations of the differences and similarities between the estimated graphs. The symmetric difference between the glasso and nonparanormal graphs is shown in (a), and the edges common to the graphs are shown in (b). Similarly, the symmetric difference between the nonparanormal and forest density estimate is shown in (c), and the common edges are shown in (d).

functions (two-way interactions) and so on.

$$\begin{aligned}
 \log p(x) &= f(x) \\
 (6.1) \quad &\equiv c + \sum_{j=1}^d f_j(x_j) + \sum_{j < k} f_{jk}(x_j, x_k) + \dots
 \end{aligned}$$

The component functions satisfy certain constraints so that the model is identifiable. In high dimensions, the model is truncated up to second order interactions so that the computation is still tractable. There is a close connection between the log-density ANOVA model and undirected graphical models. For a model with only main effects and two-way interactions, we define a graph $G = (V, E)$ such that $(i, j) \in E$ if and only if $f_{ij} \neq 0$. It can be seen that $p(x)$ is Markov to G . Jeon and Lin (2006) assume that these component functions belong to certain reproducing kernel Hilbert spaces (RKHSs) equipped with a RKHS norm $\|\cdot\|_K$. To obtain a sparse estimation of the component functions $f(x)$, they propose a penalized M-estimator,

$$\begin{aligned}
 \hat{f} = \arg \max_f &\left\{ \frac{1}{n} \sum_{i=1}^n \exp(f(X^{(i)})) \right. \\
 (6.2) \quad &\left. + \int f(x)\rho(x) dx + \lambda J(f) \right\},
 \end{aligned}$$

where $\rho(x)$ is some pre-defined positive density, and $J(f)$ is a sparsity-inducing penalty that takes the form

$$(6.3) \quad J(f) = \sum_{j=1}^d \|f_j\|_K + \sum_{j < k} \|f_{jk}\|_K.$$

Solving (6.2) only requires one-dimensional integrals which can be efficiently computed. However, the optimization in (6.2) exploits a surrogate loss instead of the log-likelihood loss, and is more difficult to analyze theoretically.

Another related idea is to conduct structure learning using nonparametric decomposable graphical models (Schwaighofer et al., 2007). A distribution is a decomposable graphical model if it is Markov to a graph $G = (V, E)$ which has a junction tree representation, which can be viewed as an extension of tree-based graphical models. A junction tree yields a factorized form

$$(6.4) \quad p(x) = \frac{\prod_{C \in V_T} p(x_C)}{\prod_{S \in E_T} p(x_S)},$$

where V_T denotes the set of cliques in V , and E_T is the set of separators, that is, the intersection of two neighboring cliques in the junction tree. Exact search for the

junction tree structure that maximizes the likelihood is usually computationally expensive. Schwaighofer et al. (2007) propose a forward-backward strategy for nonparametric structure learning. However, such a greedy procedure does not guarantee that the global optimal solution is found, and makes theoretical analysis challenging.

7. DISCUSSION

This paper has considered undirected graphical models for continuous data, where the general densities take the form

$$(7.1) \quad p(x) \propto \exp\left(\sum_{C \in \text{Cliques}(G)} f_C(x_C)\right).$$

Such a general family is at least as difficult as the general high-dimensional nonparametric regression model. But, as for regression, simplifying assumptions can lead to tractable and useful models. We have considered two approaches that make very different tradeoffs between statistical generality and computational efficiency. The nonparanormal relies on estimating one-dimensional functions, in a manner that is similar to the way additive models estimate one-dimensional regression functions. This allows arbitrary graphs, but the distribution is semiparametric, via the Gaussian copula. At the other extreme, when we restrict to acyclic graphs we can have fully nonparametric bivariate and univariate marginals. This leverages classical techniques for low-dimensional density estimation, together with approximation algorithms for constructing the graph. Clearly these are just two among many possibilities for nonparametric graphical modeling. We conclude, then, with a brief description of a few potential directions for future work.

As we saw with the nonparanormal, if only the graph is of interest, it may not be important to estimate the functions accurately. More generally, to estimate the graph it is not necessary to estimate the density. One of the most effective and theoretically well-supported methods for estimating Gaussian graphs is due to Meinshausen and Bühlmann (2006). In this approach, we regress each variable X_j onto all other variables $(X_k)_{k \neq j}$ using the lasso. This directly estimates the set of neighbors $\mathcal{N}(j) = \{k | (j, k) \in E\}$ for each node j in the graph, but the covariance matrix is *not* directly estimated. Lasso theory gives conditions and guarantees on these variable selection problems. This approach was adapted to the discrete case by Ravikumar, Wainwright and Lafferty (2010), where

the normalizing constant and thus the density can't be efficiently computed. This general strategy may be attractive for graph selection in nonparametric graphical models. In particular, each variable could be regressed on the others using a nonparametric regression method that performs variable selection; one such method with theoretical guarantees is due to Lafferty and Wasserman (2008).

A different framework for nonparametricity involves conditioning on a collection of observed explanatory variables Z . Liu et al. (2010) develop a nonparametric procedure called *Graph-optimized CART*, or *Go-CART*, to estimate the graph conditionally under a Gaussian model. The main idea is to build a tree partition on the Z space just as in CART (classification and regression trees), but to estimate a graph at each leaf using the glasso. Oracle inequalities on risk minimization and model selection consistency were established for Go-CART by Liu et al. (2010). When Z is time, graph-valued regression reduces to the time-varying graph estimation problem (Chen et al., 2010; Kolar et al., 2010; Zhou, Lafferty and Wasserman, 2010).

Another fruitful direction is the introduction of latent variables. Even though the graphical model of the observed variables X may be complex, when conditioned on some latent explanatory variables Z , the graph may be simplified. One straightforward approach is to build mixtures of the models we consider here. A mixture of nonparanormals will require new methods, to compute the derivatives $f'_j(x_j)$. A mixture of forests could be implemented using a kind of nonparametric EM algorithm, with kernel density estimates over weighted data in the M-step. But it is not easy to read off a graph from a mixture model.

In parametric settings, Chandrasekaran, Parrilo and Willsky (2010) and Choi et al. (2010) develop algorithms and theory for learning graphical models with latent variables. The first paper assumes the joint distribution of the observed and latent variables is a Gaussian graphical model, and the second paper assumes the joint distribution is discrete and factors according to a forest. Since the nonparanormal and forest density estimator are nonparametric versions of the Gaussian and forest graphical models for discrete data, we expect similar techniques to those of Chandrasekaran, Parrilo and Willsky (2010), Choi et al. (2010) can be used to extend our methods to handle latent variables. It would also be of interest to formulate nonparametric extensions of low rank plus sparse covariance matrices.

No matter how the methodology develops, nonparametric graphical models will at best be approximations

to the true distribution in many applications. Yet, there is plenty of experience to show how incorrect models can be useful. An ongoing challenge in nonparametric graphical modeling will be to better understand how the structure can be accurately estimated even when the model is wrong.

REFERENCES

- BANERJEE, O., EL GHAOU, L. and D'ASPREMONT, A. (2008). Model selection through sparse maximum likelihood estimation for multivariate Gaussian or binary data. *J. Mach. Learn. Res.* **9** 485–516. MR2417243
- CHANDRASEKARAN, V., PARRILO, P. A. and WILLSKY, A. S. (2010). Latent variable graphical model selection via convex optimization. Available at <http://arxiv.org/abs/1008.1290>.
- CHEN, X., LIU, Y., LIU, H. and CARBONELL, J. G. (2010). Learning spatial-temporal varying graphs with applications to climate data analysis. In AAAI-10: *Twenty-Fourth Conference on Artificial Intelligence* (AAAI) AAAI Press, Menlo Park, CA.
- CHOI, M. J., TAN, V. Y., ANANDKUMAR, A. and WILLSKY, A. S. (2010). Learning latent tree graphical models. Available at <http://arxiv.org/abs/1009.2722>.
- CHOW, C. and LIU, C. (1968). Approximating discrete probability distributions with dependence trees. *IEEE Transactions on Information Theory* **14** 462–467.
- FRIEDMAN, J. H., HASTIE, T. and TIBSHIRANI, R. (2007). Sparse inverse covariance estimation with the graphical lasso. *Biostatistics* **9** 432–441.
- GINÉ, E. and GUILLOU, A. (2002). Rates of strong uniform consistency for multivariate kernel density estimators. *Ann. Inst. H. Poincaré Probab. Stat.* **38** 907–921. MR1955344
- JEON, Y. and LIN, Y. (2006). An effective method for high-dimensional log-density ANOVA estimation, with application to nonparametric graphical model building. *Statist. Sinica* **16** 353–374. MR2267239
- KOLAR, M., SONG, L., AHMED, A. and XING, E. P. (2010). Estimating time-varying networks. *Ann. Appl. Stat.* **4** 94–123. MR2758086
- KRUSKAL, J. B. JR. (1956). On the shortest spanning subtree of a graph and the traveling salesman problem. *Proc. Amer. Math. Soc.* **7** 48–50. MR0078686
- LAFFERTY, J. and WASSERMAN, L. (2008). Rodeo: Sparse, greedy nonparametric regression. *Ann. Statist.* **36** 28–63. MR2387963
- LIU, H., LAFFERTY, J. and WASSERMAN, L. (2009). The nonparanormal: Semiparametric estimation of high dimensional undirected graphs. *J. Mach. Learn. Res.* **10** 2295–2328. MR2563983
- LIU, H., CHEN, X., LAFFERTY, J. and WASSERMAN, L. (2010). Graph-valued regression. In *Proceedings of the Twenty-Third Annual Conference on Neural Information Processing Systems (NIPS)*.
- LIU, H., XU, M., GU, H., GUPTA, A., LAFFERTY, J. and WASSERMAN, L. (2011). Forest density estimation. *J. Mach. Learn. Res.* **12** 907–951. MR2786914
- LIU, H., HAN, F., YUAN, M., LAFFERTY, J. and WASSERMAN, L. (2012). High dimensional semiparametric Gaussian

- copula graphical models. In *Proceedings of the 29th International Conference on Machine Learning (ICML-12)*. ACM, New York.
- MALLOWS, C. L., ed. (1990). *The Collected Works of John W. Tukey. Vol. VI: More Mathematical: 1938–1984*. Wadsworth & Brooks/Cole Advanced Books & Software, Pacific Grove, CA. [MR1057793](#)
- MEINSHAUSEN, N. and BÜHLMANN, P. (2006). High-dimensional graphs and variable selection with the lasso. *Ann. Statist.* **34** 1436–1462. [MR2278363](#)
- RAVIKUMAR, P., WAINWRIGHT, M. J. and LAFFERTY, J. D. (2010). High-dimensional Ising model selection using ℓ_1 -regularized logistic regression. *Ann. Statist.* **38** 1287–1319. [MR2662343](#)
- RAVIKUMAR, P., WAINWRIGHT, M., RASKUTTI, G. and YU, B. (2009). Model selection in Gaussian graphical models: High-dimensional consistency of ℓ_1 -regularized MLE. In *Advances in Neural Information Processing Systems*, **22** MIT Press, Cambridge, MA.
- ROTHMAN, A. J., BICKEL, P. J., LEVINA, E. and ZHU, J. (2008). Sparse permutation invariant covariance estimation. *Electron. J. Stat.* **2** 494–515. [MR2417391](#)
- SCHWAIGHOFER, A., DEJORI, M., TRESP, V. and STETTER, M. (2007). Structure learning with nonparametric decomposable models. In *Proceedings of the 17th International Conference on Artificial Neural Networks. ICANN'07*. Elsevier, New York.
- SKLAR, M. (1959). Fonctions de répartition à n dimensions et leurs marges. *Publ. Inst. Statist. Univ. Paris* **8** 229–231. [MR0125600](#)
- WASSERMAN, L. (2006). *All of Nonparametric Statistics*. Springer, New York. [MR2172729](#)
- WILLE, A., ZIMMERMANN, P., VRANOVÁ, E., FÜRHOZ, A., LAULE, O., BLEULER, S., HENNIG, L., PRELIĆ, A., VON ROHR, P., THIELE, L., ZITZLER, E., GRUISSEM, W. and BÜHLMANN, P. (2004). Sparse Gaussian graphical modelling of the isoprenoid gene network in *Arabidopsis thaliana*. *Genome Biology* **5** R92.
- YUAN, M. and LIN, Y. (2007). Model selection and estimation in the Gaussian graphical model. *Biometrika* **94** 19–35. [MR2367824](#)
- ZHOU, S., LAFFERTY, J. and WASSERMAN, L. (2010). Time varying undirected graphs. *Mach. Learn.* **80** 295–329.